Modelling Power Amplifier Impairments in mmWave Phased-Array Systems

Nebojsa Maletic and Eckhard Grass

This letter presents an analytical framework to study the distortion effect of power amplifiers (PA) in a single-stream millimetre wave (mmWave) system with a radio-frequency (RF) beamforming architecture. A third-order nonlinearity PA model is used. The impact of PA nonlinearity on the transmitter performance is evaluated by means of its normalised mean square error (NMSE). Also, the effect of PA compression on the system capacity in a line-of-sight (LOS) channel is analysed. All analytical results are supported with Monte-Carlo simulations.

Introduction: In recent years millimetre wave (mmWave) communication has gained significant research interest. It is regarded as a pivotal technology to accommodate high data rates [1]. Although able to support high capacities thanks to large bandwidths, the mmWave frequencies exhibit a high path loss. Therefore, mmWave transceivers employ large phased-arrays to generate beamforming gains and to improve the link budget [2]. In addition, high capacities and large bandwidths pose stringent requirements, among others, on the tolerable amount of radio-frequency (RF) impairments.

The number of papers studying the effects of RF impairments on the performance of a single-stream mmWave RF beamforming system is sparse. The influence of phase noise and different local-oscillator (LO) architectures on the performance of mmWave systems with a hybrid beamforming architecture is studied in [3]. In the form of residual distortion noise, the impact of transmitter impairments on the capacity performance of mmWave systems with RF and hybrid beamforming architectures is investigated in [4]. For the former, an upper bound of capacity in a non-line-of-sight (NLOS) channel is provided. In [5], the influence of both transmitter and receiver residual distortion noises in a single-stream mmWave RF beamforming system is studied. The authors employ an equivalent single antenna model to derive a closed-form expression for ergodic capacity in both LOS and NLOS channels. While, in the latter systems, the effects of phase noise or IQ mismatch can be analysed similarly to a single antenna system, the same approach cannot be straightforwardly applied to the power amplifier (PA) compression effects. The main reason is that the signals in the branches of an antenna array cannot be considered uncorrelated.

Therefore, in this letter, we study the impact of PA nonlinearity in a multi-antenna system employing an RF beamforming transceiver architecture. Such an architecture is typical for mmWave transceivers. Using a third-order nonlinearity model, we investigate the effect of PA compression on transmitter performance. Furthermore, the same effect on the capacity of the system in an LOS channel is assessed.

A PA distortion-aware transmitter model: A block diagram of a mmWave phased-array transmitter is shown in Fig. 1. The transmitter employs an RF beamforming architecture, having N_t antenna branches so that each branch comprises a phase shifter and a power amplifier. Furthermore, we assume that the signal at the input of the transmitter s is

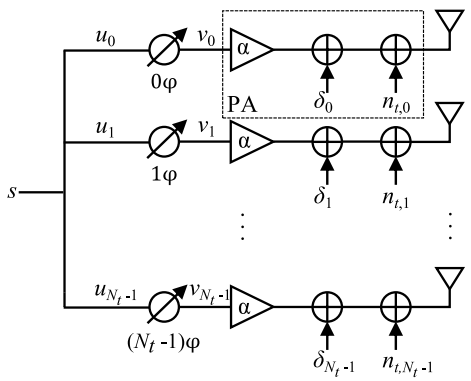

Fig. 1 *An illustration of a mmWave phased-array transmitter including power amplifier impairments*

a zero-mean circular complex-Gaussian random variable with variance $\mathtt{E}[ss^*]=\sigma_s^2$, i.e., $s\sim\mathcal{CN}(0,\sigma_s^2)$. Note that this assumption holds for orthogonal frequency division multiplexing (OFDM) modulated signals. For beamforming, the transmitter employs a transmit beamforming vector $\mathbf{f}$

$$\mathbf{f}=\begin{bmatrix}f_0 & f_1 & \dots & f_{N_t-1}\end{bmatrix}^T=\frac{1}{\sqrt{N_t}}\begin{bmatrix}1 & e^{j\varphi} & \dots & e^{j(N_t-1)\varphi}\end{bmatrix}^T \tag{1}$$

where $f_l=e^{jl\varphi}/\sqrt{N_t}$ with φ being a phase shift. The factor $N_t^{-1/2}$ allows $\mathbf{f}$ having the unit norm.

The transmitter is driven by the signal s, being first ideally up-converted, and then (power) divided into N_t copies, such that each copy feeds one branch of the phased-array. The input signal of the l-th branch is $u_l=\frac{s}{\sqrt{N_t}}$, $l=0,1,...,N_t-1$, with variance $\mathtt{E}\left[u_l u_l^*\right]=\sigma_{u_l}^2=\sigma_s^2/N_t$. Hence, $u_l\sim\mathcal{CN}(0,\sigma_{u_l}^2)$. The signal u_l is then shifted in phase, yielding the signal $v_l=u_l\cdot e^{jl\varphi}$, such that $v_l=f_l s$. Note that v_l is also a zero-mean circular complex-Gaussian random variable, having the same variance as u_l, i.e. $\sigma_{v_l}^2=\sigma_{u_l}^2=\sigma_s^2/N_t$ [6].

After the phase shifting process, the signal v_l drives a PA yielding the output [7]

$$x_l=r(v_l)+n_{t_l} \tag{2}$$

$r(\cdot)$ represents a nonlinear function used to describe PA nonlinearity (i.e., compression). The second term describes the output thermal noise that can be modeled as a zero-mean complex-Gaussian random variable with variance $\mathtt{E}\left[n_{t_l}n_{t_l}^*\right]=\sigma_{n_t}^2$.

Using Busgang's theorem [8], the output of a circuit exhibiting nonlinearity can be expressed as a sum of the attenuated input signal replica and the distortion noise δ_l

$$r_l=\alpha v_l+\delta_l \tag{3}$$

Note that δ_l is not independent of v_l, however, both are jointly uncorrelated. In this work, we consider a third-order nonlinearity model of the PA. Further, we assume that PAs are the same in all branches of the beamforming transceiver, which is a reasonable assumption for chip-integrated beamformers. For the above-mentioned PA model, the input-output relationship reads [7]

$$r(v_l)=v_l+\rho v_l|v_l|^2 \tag{4}$$

where $\rho\in\Re$, $\rho<0$ denotes the compression parameter. Owing to [7], the 1-dB compression point is approximately equal to $\sigma_{v_l,1dB}^2\approx 0.056|\rho|^{-1}$ or $\sigma_{s,1dB}^2\approx 0.056|\rho|^{-1}N_t$. From (3) and (4), the Busgang's attenuation factor α can be derived as [7]

$$\alpha\triangleq\frac{\mathtt{E}\left[r_l v_l^*\right]}{\mathtt{E}\left[v_l v_l^*\right]}=1+2\rho\mathtt{E}\left[v_l v_l^*\right]=1+2\rho\frac{\sigma_s^2}{N_t} \tag{5}$$

The variance of the l-th branch distortion noise δ_l can be expressed as [9]

$$\sigma_\delta^2=\mathtt{E}\left[\delta_l\delta_l^*\right]=2\rho^2\mathtt{E}\left[v_l v_l^*\right]^3=2\rho^2\frac{\sigma_s^6}{N_t^3} \tag{6}$$

For other PA models (SEL, TWTA, SSPA or memoryless polynomial), the attenuation factor and the variance of distortion noise can be found in [10] - [13].

The distortion noises between branches of the beamforming transmitter are not uncorrelated because their input signals originate from the same source. The cross-covariance of distortion noises between the l-th and k-th branches can be found [7]

$$\mathtt{E}\left[\delta_l\delta_k^*\right]=2\rho^2\mathtt{E}\left[v_l v_k^*\right]\left|\mathtt{E}\left[v_l v_k^*\right]\right|^2=2\rho^2 e^{j(l-k)\varphi}\frac{\sigma_s^6}{N_t^3} \tag{7}$$

Clearly, the correlation coefficient ζ has a unit-magnitude and phase $\angle\zeta=(l-k)\varphi$.

Finally, by combining all the aforementioned, the signal emitted from the l-th antenna can be written as

$$x_l=\frac{\alpha}{\sqrt{N_t}}e^{jl\varphi}s+\delta_l+n_{t_l}=\alpha f_l s+\delta_l+n_{t_l} \tag{8}$$

and the total (power combined) transmitted signal reads

$$\mathbf{x}=\alpha\mathbf{f}s+\boldsymbol{\Delta}+\mathbf{n}_t \tag{9}$$

where $\mathbf{\Delta} = \begin{bmatrix}\delta_0 & \delta_1 & ... & \delta_{N_t-1}\end{bmatrix}^T$ is the distortion noise vector with covariance matrix given as $\mathtt{E}\left[\mathbf{\Delta}\mathbf{\Delta}^H\right] = 2\rho^2\sigma_s^6 N_t^{-2}\mathbf{f}\mathbf{f}^H$. The variance of the transmitter noise vector is $\mathtt{E}\left[\mathbf{n}_t\mathbf{n}_t^H\right] = \sigma_{n_t}^2\mathbf{I}_{N_t}$. In the ideal case (no PA impairments), the signal reads $\mathbf{x}_o = \mathbf{f}s$.

NMSE of the transmitter: The performance of a phased-array transmitter under PA impairments is evaluated by means of the normalised mean squared error (NMSE). The NMSE of the l-th branch is defined as [7]

$$\mathtt{NMSE}_l \triangleq \frac{\mathtt{E}\left[e_l e_l^*\right]}{\mathtt{E}\left[x_{o,l}x_{o,l}^*\right]} = N_t\frac{\sigma_e^2}{\sigma_s^2} \tag{10}$$

where σ_e^2 is the variance of the error $e_l = x_l - x_{o,l} = (\alpha-1)f_l s + \delta_l + n_{t_l}$ and σ_s^2 is the variance of the ideally transmitted signal. After finding the power of each term in the error signal, it can be shown that the final expression takes the following form

$$\mathtt{NMSE}_l = 2\rho^2\frac{\sigma_s^4}{N_t^2} + N_t\frac{\sigma_{n_t}^2}{\sigma_s^2} = 2\rho^2 N_t^{-2}\sigma_s^4 + N_t\mathtt{SNR_t}^{-1} \tag{11}$$

where $\mathtt{SNR}_t = \sigma_s^2/\sigma_{n_t}^2$ denotes the transmitter signal-to-noise ratio (SNR). Similar to [9], the optimal signal power, which minimises the NMSE, is found as

$$\bar{\sigma}_s^2 = \arg\min_{\sigma_s^2}\mathtt{NMSE}_l = N_t\sqrt[3]{\frac{\sigma_{n_t}^2}{12\rho^2}} \tag{12}$$

The NMSE in (11) can be related to the error-vector magnitude (EVM) as follows $\mathtt{EVM}^2 = \mathtt{NMSE}_l$. The EVM is another figure of merit used to quantify the quality of an RF transceiver.

Capacity: Next, we investigate the impact of PA distortion noise on capacity. We assume that the communication takes place in an LOS channel, with the channel matrix expressed as

$$\mathbf{H} = \beta\mathbf{a}_r(\theta)\mathbf{a}_t^H(\phi) \tag{13}$$

β is the gain of the LOS path, satisfying $\beta \sim \mathcal{CN}(0,\sigma_\beta^2)$, and θ and ϕ are azimuths angle of arrival (AoA) and angle of departure (AoD), respectively, given as $\theta = \frac{2d}{\lambda}\sin(\Theta)$ and $\phi = \frac{2d}{\lambda}\sin(\Phi)$, with Θ and Φ being the physical AoA and AoD in the range [$-\pi/2, \pi/2$]. λ is the carrier wavelength and $d = \lambda/2$ is the inter-antenna spacing. $\mathbf{a}_t$ and $\mathbf{a}_r$ are the array response vectors at the transmitter and the receiver, respectively. For a uniform linear array (ULA) with N antennas, the array response vector reads [14]

$$\mathbf{a}(\phi) = \frac{1}{\sqrt{N}}\left[1, e^{j\pi\phi}, ..., e^{j(N-1)\pi\phi}\right]^T \tag{14}$$

Under the assumption of perfect synchronisation, the received signal is

$$y = \sigma_a\mathbf{w}^H\mathbf{H}\mathbf{x} + \mathbf{w}^H\mathbf{n}_r \tag{15}$$

where $\sigma_a^2 = (\lambda/4\pi D)^2$ is the free-space path loss induced attenuation, D is the distance. $\mathbf{w}$ is the unit-norm receive beamforming vector as in (1) and $\mathbf{n}_r$ is the receiver noise vector with variance $\mathtt{E}\left[\mathbf{n}_r\mathbf{n}_r^H\right] = \sigma_{n_r}^2\mathbf{I}_{N_r}$. After combining (9) and (15), we obtain

$$y = \sigma_a\alpha\mathbf{w}^H\mathbf{H}\mathbf{f}s + \sigma_a\mathbf{w}^H\mathbf{H}\mathbf{\Delta} + \sigma_a\mathbf{w}^H\mathbf{H}\mathbf{n}_t + \mathbf{w}^H\mathbf{n}_r \tag{16}$$

The first term is the useful signal, the second term denotes the distortion noise due to PA compression and the remaining are transmitter and receiver thermal noises. Then, the signal-to-noise-distortion ratio (SNDR) can be expressed as

$$SNDR = \frac{\alpha^2\mathtt{E}_s\left[|\mathbf{w}^H\mathbf{H}\mathbf{f}s|^2\right]}{\mathtt{E}_{\mathbf{\Delta}}\left[|\mathbf{w}^H\mathbf{H}\mathbf{\Delta}|^2\right] + \mathtt{E}_{\mathbf{n}_t}\left[|\mathbf{w}^H\mathbf{H}\mathbf{n}_t|^2\right] + \sigma_a^{-2}\mathtt{E}_{\mathbf{n}_r}\left[|\mathbf{w}^H\mathbf{n}_r|^2\right]}$$
$$= \frac{\alpha^2\sigma_s^2\eta_t\eta_r\beta^2}{2\rho^2 N_t^{-2}\sigma_s^6\eta_t\eta_r\beta^2 + \sigma_{n_t}^2\eta_r\beta^2 + \sigma_a^{-2}\sigma_{n_r}^2} \tag{17}$$

The above expression represents an instantaneous SNDR, which depends on the current channel power β^2, $\beta^2 \sim \mathrm{Exp}(\sigma_\beta^{-2})$. Mathematically, the average SNDR can be found by taking the expectation of (17), $\mathrm{SNDR} = \mathtt{E}_{\beta^2}\left[SNDR\right]$. The analytic solution is feasible, but it was found out that the function is not defined for all values of the argument. Therefore, the average SNDR is approximated, with the help of [11, eq. (29)], i.e. $\mathrm{SNDR} \approx \mathtt{E}\left[x\right]/\mathtt{E}\left[y\right]$, to (18). There is a small difference between the exact and approximate solution but this will not affect the reached conclusions.

$$\mathtt{SNDR} \simeq \frac{\alpha^2\sigma_\beta^2\sigma_s^2\eta_t\eta_r}{2\rho^2 N_t^{-2}\sigma_\beta^2\sigma_s^6\eta_t\eta_r + \sigma_\beta^2\sigma_{n_t}^2\eta_r + \sigma_a^{-2}\sigma_{n_r}^2} =$$
$$= \frac{\alpha^2\eta_t\eta_r\mathtt{SNR}}{2\rho^2 N_t^{-2}\sigma_s^4\eta_t\eta_r\mathtt{SNR} + \eta_r\mathtt{SNR}_t^{-1}\mathtt{SNR} + 1} \tag{18}$$

In (18) $\mathtt{SNR} = \sigma_\beta^2\sigma_s^2/\sigma_a^{-2}\sigma_{n_r}^2$ denotes the SNR in the ideal case. The parameters η_t and η_r denote the Fejér kernels [5] at the transmitter and the receiver, respectively. When the directions of transmit and receive beamforming vectors are aligned with AoD and AoA, then $\eta_t = \eta_r = 1$; otherwise, they are

$$\eta_t = \frac{1}{N_t^2}\left|\frac{\sin\frac{\pi(\phi-\varphi_t)N_t}{2}}{\sin\frac{\pi(\phi-\varphi_t)}{2}}\right|^2, \eta_r = \frac{1}{N_r^2}\left|\frac{\sin\frac{\pi(\theta-\varphi_r)N_r}{2}}{\sin\frac{\pi(\theta-\varphi_r)}{2}}\right|^2 \tag{19}$$

If AoA (or AoD) is uniformly distributed in the azimuth range of interest, it was shown in [5] that the expected value of the Fejér kernel can be approximated to 0.77935.
Finally, the capacity is obtained as $C = \log_2(1+\mathtt{SNDR})$. It is maximised when SNDR in (18) has its maximum; the optimal power is found by

$$\tilde{\sigma}_s^2 = \arg\max_{\sigma_s^2}\mathtt{SNDR} \tag{20}$$

The final expression is cumbersome and thus omitted, but it can be obtained using a symbolic solver from, e.g., *Mathematica*. Another way to solve (20) is a one-dimensional numerical search. Having the optimal signal power $\tilde{\sigma}_s^2$, the optimal capacity is given by

$$C_{opt} = \log_2\left(1 + \mathtt{SNDR}(\tilde{\sigma}_s^2)\right) \tag{21}$$

It should be noted that the capacity C can be zero when $\sigma_s^2 = N_t/(2|\rho|)$. Besides, it can be shown that, in the high power region ($\sigma_s^2 \gg N_t/(2|\rho|)$, SNDR tends to 2 and the capacity approaches $C_\infty = \log_2(3) \approx 1.59$ b/s in 1 Hz of bandwidth. This behaviour is due to the nature of the used PA model.

Numerical results: A numerical example illustrates the effects of PA compression on the system performance. For that purpose, the compression parameter is set to $\rho = -0.05$, and the transmitter noise power is -50 dBm. The former can be obtained from large-signal gain parameters such as the third-order intercept and 1-dB compression points. The latter can be calculated from the output noise power spectral density integrated over channel bandwidth. For example, assuming a 2 GHz wide channel (e.g., in the 60 GHz band) and an optimistic output noise spectral density of -143 dBm/Hz, the noise power equals -50 dBm. We set $D = 10$ m and $\lambda = 5$ mm. The noise power is calculated as $\sigma_{n_r}^2 = FkTB$ where $F = 10$ denotes the noise factor, $k = 1.38\cdot 10^{-23}$ J/K, $T = 290$ K and $B = 2$ GHz. Moreover, we consider an equal number of antennas at both transmitter and receiver $N_t = N_r = N = \{16, 32, 64\}$. Besides, we set $\sigma_\beta^2 = N_t N_r$ to keep $||\mathbf{H}||_F^2 = N_t N_r$. We performed 10^5 simulation runs.

The NMSE of a single branch of the phased-array transmitter is shown in Fig. 2. There is an optimal signal power that minimises the NMSE, which equals $0.45, 3.46, 6.47$ dBm for $N = \{16, 32, 64\}$, respectively. The optimal power increases when larger arrays are employed. Also, when the transmitter operates with higher signal powers σ_s^2, e.g., in the 1-dB compression region, the NMSE performance deteriorates.

The influence of PA compression on capacity is depicted in Fig. 3. There is an optimal signal power that maximises the capacity, and this power is independent of the array size N. Moreover, the capacity-optimal signal power is higher than the NMSE-optimal signal power, as shown in Fig. 3, and is located in the 1-dB compression region (more precisely, in this example, near 1-dB compression point for $N = 16$, ≈ 12.5 dBm). Hence, when the NMSE-optimal beamforming transmitter is used, the maximum system capacity is not reached. This means, in other words, that both figures of merit are not simultaneously optimised. In Fig. 3, we also compared the case when both transmitter and receiver can perfectly align their beams with respect to the channel AoD and AoA (solid curves) to the case when both have a finite number of beamforming directions (dashed curves), which would be the case in practice. To illustrate the difference, we employed an N-DFT beambook. In the latter case, the

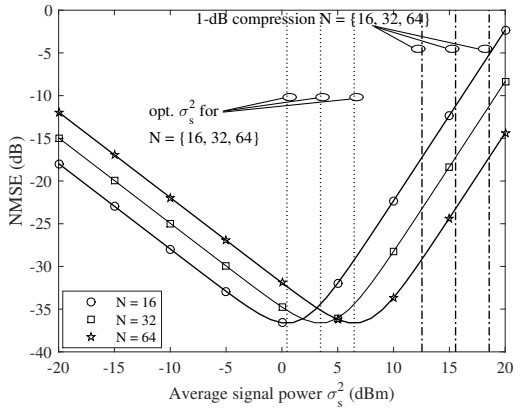

Fig. 2 *Normalised mean square error (NMSE) of a phased-array transmitter* $N = \{16, 32, 64\}$

Simulation results are illustrated by markers. Analytical results are shown with solid lines. For convenience, the NMSE-optimal and 1-dB compression signal powers are plotted.

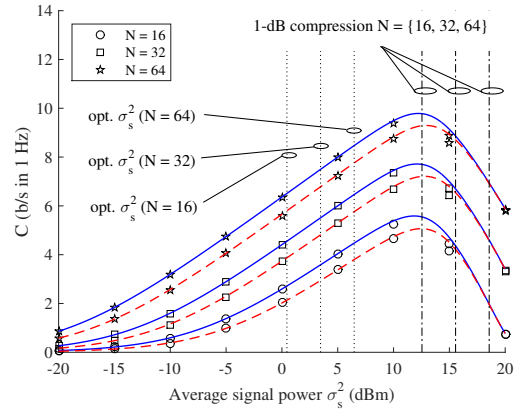

Fig. 3 *Capacity of a single-stream mmWave beamforming system for* $N = \{16, 32, 64\}$

Simulation results are illustrated by markers. Analytical results are shown with solid and dashed lines. There is a small difference between the two in the peak region due to (18) being approximate. For convenience, the NMSE-optimal and 1-dB compression signal powers are plotted.

capacity is slightly lower because of imperfect alignment. The difference, i.e., the capacity loss is illustrated in Fig. 4. The capacity loss has a "pulse-like" shape, which broadens and grows with bigger N (because of higher beamforming gain). For $N = 64$, it reaches a peak of around 0.7 b/s in 1 Hz. In the high power region, the curves almost overlap, and the loss drops because of the dominant effect of PA compression.

Conclusion: We have derived some results on the effects of power amplifier (PA) nonlinearity in millimetre wave (mmWave) phased-array systems employing a radio-frequency (RF) beamforming architecture. The transmitter has been analysed in terms of normalised mean square error (NMSE) performance. The outcome implies, there is an optimal signal power for minimal NMSE, dependent on the array size. Furthermore, the impact of PA compression on the capacity performance has been investigated, showing an optimal signal power maximises the capacity but it differs from the optimal point for the NMSE. Hence, increasing the transmitter output power by a limited amount beyond the optimum NMSE point, can be useful to achieve higher or even optimum system capacity. Finally, we see the derived analytical expressions as a useful tool to evaluate the performance of phased-array systems under consideration of PA compression and to balance various parameters and design aspects effectively.

Acknowledgment: The work of N. Maletic has been supported by the European Union's H2020 research and innovation programme under Grant Agreement No. 815178 (5GENESIS). The work of E. Grass has been supported by the German Research Foundation (DFG) within the project Agile-HyBeamS (DFG No. 421544431).

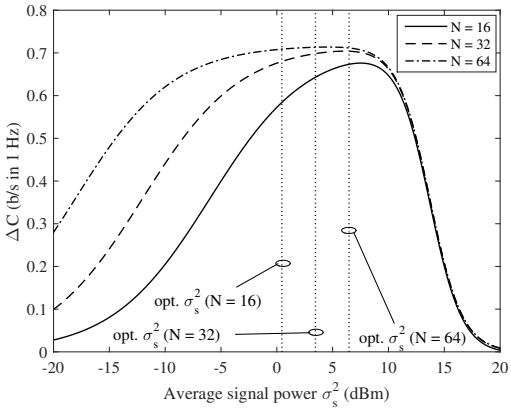

Fig. 4 *Capacity loss due to a finite number of beamforming directions for* $N = \{16, 32, 64\}$

The NMSE-optimal signal powers are shown for convenience.

Nebojsa Maletic and Eckhard Grass (*IHP – Leibniz-Institut für innovative Mikroelektronik, Frankfurt (Oder), Germany*)

E-mail: maletic@ihp-microelectronics.com

Eckhard Grass: also with Humboldt-Universität zu Berlin, Berlin, Germany

No data available. The authors declare that they have no competing interests.

References

1 W. Roh, J.-Y. Seol, J. Park, B. Lee, J. Lee, Y. Kim, J. Cho, K. Cheun and F. Aryanfar, 'Millimeter-wave beamforming as an enabling technology for 5G cellular communications: theoretical feasibility and prototype results,' *IEEE Commun. Mag.*, **52**, p. 106–113, 2014

2 T. Rappaport, R. W. Heath Jr., T. Daniels and J. Murdock, 'Millimeter wave wireless communications', *Prentice Hall*, 2014

3 M. U. Aminu, J. Lehtomäki and M. Juntti, 'Beamforming and Transceiver Optimization with Phase Noise for mmWave and THz Bands,' *2019 16th International Symposium on Wireless Communication Systems (ISWCS)*, Oulu, Finnland, 2019, p. 436–440

4 N. Maletic, J. Gutiérrez-Teran and E. Grass, 'Beamforming mmWave MIMO: Impact of Nonideal Hardware and Channel State Information,' *2018 26th Telecommunications Forum (TELFOR)*, Belgrade, 2018, p. 1-6. doi: 10.1109/TELFOR.2018.8611829

5 N. Maletic, J. Gutiérrez and E. Grass, 'On the Impact of Residual Transceiver Impairments in mmWave RF Beamforming Systems,' *IEEE Commun. Lett.*, **24**, p. 2459–2463, Nov. 2020, doi: 10.1109/LCOMM.2020.3013171.

6 D. Tse, P. Wiswanath, 'Fundamentals of Wireless Communication,' *Cambridge University Press*, 2005

7 P. Händel and D. Rönnew, 'Dirty MIMO Transmitters: Does It Matter?,' *IEEE Trans. Wirel. Commun.*, **17**, p. 5425–5436, Aug. 2018

8 N. Y. Ermolova and S. G. Haggman, 'An extension of Bussgang's theory to complex-valued signals,' *Proceedings of the 6th Nordic Signal Processing Symposium, 2004. NORSIG 2004.*, Espoo, Finland, 2004, p. 45–48.

9 P. Händel and D. Rönnew, 'Modeling Mixer and Power Amplifier Impairments,' *IEEE Microw. Wirel. Compon. Lett.*, **29**, 2019

10 N. Maletic, M. Cabarkapa, N. Neskovic and D. Budimir, 'Hardware impairments impact on fixed-gain AF relaying performance in Nakagami-m fading,' *IET Electron. Lett.*, **52**, p. 121–122, 21 1 2016, doi: 10.1049/el.2015.3378.

11 N. Maletic, M. Cabarkapa and N. Neskovic, 'Performance of fixed-gain amplify-and-forward nonlinear relaying with hardware impairments,' *Int. J. of Commun. Syst.*, **30**, 2017

12 E. Balti and M. Guizani, 'Impact of Non-Linear High Power Amplifiers on Cooperative Relaying Systems', *IEEE Trans. Commun.*, 10.1109/TCOMM.2017.2722499, 2017.

13 T. Schenk, 'RF Imperfections in High-Rate Wireless Systems: Impact and Digital Compensation', *Springer: Netherlands*, 2008

14 Z. Xiao, T. He, P. Xia and X. Xia, 'Hierarchical Codebook Design for Beamforming Training in Millimeter-Wave Communication,' *IEEE Trans. Wirel. Commun.*, **15**, p. 3380–3392, May 2016. doi: 10.1109/TWC.2016.2520930